Journal of Power Sources 195 (2010) 2212–2219

Contents lists available at ScienceDirect

Journal of Power Sources

journal homepage: www.elsevier.com/locate/jpowsour

Quaternized poly(vinyl alcohol)/alumina composite polymer membranes for alkaline direct methanol fuel cells

Chun-Chen Yang*, Shwu-Jer Chiu, Wen-Chen Chien, Sheng-Shin Chiu

Department of Chemical Engineering, Mingchi University of Technology, 84 Gungjuan Rd., Taipei Hsien 243, Taiwan, ROC

ARTICLE INFO

Article history:
Received 10 September 2009
Received in revised form 30 October 2009
Accepted 30 October 2009
Available online 10 November 2009

Keywords:
Quaternized
PVA
Al_2O_3
Nanocomposite polymer membrane
Alkaline
Direct methanol fuel cell (DMFC)

ABSTRACT

The quaternized poly(vinyl alcohol)/alumina (designated as QPVA/Al_2O_3) nanocomposite polymer membrane was prepared by a solution casting method. The characteristic properties of the QPVA/Al_2O_3 nanocomposite polymer membranes were investigated using thermal gravimetric analysis (TGA), scanning electron microscopy (SEM), dynamic mechanical analysis (DMA), micro-Raman spectroscopy, and AC impedance method. Alkaline direct methanol fuel cell (ADMFC) comprised of the QPVA/Al_2O_3 nanocomposite polymer membrane were assembled and examined. Experimental results indicate that the DMFC employing a cheap non-perfluorinated (QPVA/Al_2O_3) nanocomposite polymer membrane shows excellent electrochemical performances. The peak power densities of the DMFC with 4 M KOH + 1 M CH_3OH, 2 M CH_3OH, and 4 M CH_3OH solutions are 28.33, 32.40, and 36.15 mW cm^{-2}, respectively, at room temperature and in ambient air. The QPVA/Al_2O_3 nanocomposite polymer membranes constitute a viable candidate for applications on alkaline DMFC.

1. Introduction

Direct methanol fuel cells (DMFCs) are recently gaining much attention for their highly potential applications on the electric vehicles (EVs), stationary applications, and portable power sources, such as cellular phones, notebook computers, etc. At the present time, direct methanol fuel cell (DMFC) is being actively studied and a lot of progress is made during the past few years [1–15]. However, the development of the DMFC has been hampered due to several serious problems, which are slow methanol oxidation kinetics and incomplete electrooxidation of methanol, the poisoning of adsorbed intermediate species on the Pt surface, the high methanol crossover through the solid-state polymer Nafion membrane, and the high costs of the Nafion (Du pont) polymer membrane and Pt catalyst.

Recently, Yang et al. [1,2] synthesized the cross-linked PVA-based composite polymer membranes and applied in an alkaline DMFC. More precisely, the carbonation problem of alkaline DMFC can be greatly reduced by using an alkaline solid polymer membrane instead of an alkaline solution [3–6]. In addition, as we know, the anodic electrooxidation of methanol in an alkaline media shows much faster kinetics than that in an acidic media [7]. The works on the preparation of the anion exchange polymer membrane for alkaline DMFC have been studied intensively [8–15]. Recently, many kinds of anion exchange polymer membrane based on quaternized polymers applied for the alkaline alcohol fuel cells have been investigated [9,15].

Interestingly, Xiong et al. [16] studied a quaternized poly(vinyl alcohol) (here designated as QPVA) polymer membrane for applications in DMFC. The quaternary ammonium groups were grafted onto the backbone of the PVA host. The ionic conductivity of QPVA exchange polymer membrane was 7.34×10^{-3} S cm^{-1} in deionized water at 30 °C. Moreover, Xiong et al. [17,18] also prepared and examined two organic–inorganic hybrid anion exchange membranes based on QPVA and tetraethoxylsilanes (TEOS) [17] and QPVA/chitosan [18]. These composite polymer membranes show a high ionic conductivity of 10^{-3} to 10^{-2} S cm^{-1} and a low methanol permeability of 5.68×10^{-7} to 4.42×10^{-6} cm^2 s^{-1} at 30 °C. However, they did not show any electrochemical data for applications in an alkaline DMFC [16–18].

There are several ceramic fillers being used on the polymer electrolyte membrane, for examples, TiO_2 [1], SiO_2 [6], α-Al_2O_3 [19], bentonite [20], which are blended into the PVA polymer. Alumina (Al_2O_3) [19] was used owing to its good physical (hydrophilic) and chemical (inert) properties. Alumina is typically used in the form of nano-particles providing with high surface area and activity, and excellent chemical stability. The addition of hydrophilic Al_2O_3 fillers into the polymer matrix reduces the crystallinity of the PVA polymer, therefore increasing the amorphous phases of PVA polymer matrix, resulting in an increase of its ionic conductivity. As we know, when Al_2O_3 filler used as a stiffener material added to the PVA matrix, the mechanical properties of the QPVA/Al_2O_3

* Corresponding author. Tel.: +886 29089899; fax: +886 29041914.
E-mail address: ccyang@mail.mcut.edu.tw (C.-C. Yang).

0378-7753/$ – see front matter © 2009 Elsevier B.V. All rights reserved.
doi:10.1016/j.jpowsour.2009.10.091

nanocomposite polymer membrane greatly enhance. The thermal property, dimensional stability, and swelling ratio could also be improved.

In this work, we attempt to disperse these nano-sized Al_2O_3 ceramic fillers into the QPVA matrix to act as a solid plasticizer capable of enhancing the chemical and thermal properties, and dimensional stability for the QPVA/Al_2O_3 nanocomposite polymer membrane. Alkaline DMFC, comprised of the air cathode loaded with MnO_2/BP2000 carbon ink on a Ni-foam, the PtRu anode based on a Ti-screen, and using a QPVA/Al_2O_3 nanocomposite polymer membrane, was assembled and investigated. The QPVA/Al_2O_3 composite polymer membrane was prepared by a direct blend of QPVA polymer (PVA being amination by GTMAC first) and nano-sized Al_2O_3 fillers under a stirring condition. A 5 wt.% glutaraldehyde (GA) solution was finally directly added to the composite polymer membrane for the cross-linking reaction. In comparison, among three methanol concentrations (1–4 M), were tested. The electrochemical characteristics of alkaline DMFC using a QPVA/Al_2O_3 nanocomposite polymer membrane were investigated by the linear polarization and galvanostatic methods; especially for the peak power density of alkaline DMFC in ambient conditions.

2. Experimental

2.1. Preparation of the QPVA/Al_2O_3 composite polymer membrane

PVA (Aldrich), nano-sized Al_2O_3 fillers (10–30 nm, 200 $m^2\,g^{-1}$, CBT, Taiwan), glycidytrimethyl ammonium chloride (GTMAC) (Aldrich), and KOH (Merck) were used as received without further purification. Degree of polymerization and saponification of PVA were 1700 and 98–99%, respectively. The QPVA/Al_2O_3 nanocomposite polymer membrane was prepared by a solution casting method [8–10].

The appropriate quantities of the PVA polymer were dissolved in distilled water under stirring. The above resulting solution was stirred continuously until the solution mixture became homogeneous with viscous appearance at 85 °C for 3 h. The temperature of the viscous mixture was cooled to 65 °C, then a suitable amount of GTMAC, KOH (GTMAC:KOH = 1:1 in mole ratio) was added to the resulting mixture solution under a continuous stirring condition for 4 h. The resulting viscous polymer mixture was washed using anhydrous alcohol to obtain yellow precipitates. Then, these quaternized poly(vinyl alcohol) precipitates (the so-called QPVA) were dried at 65 °C in a vacuum oven.

The QPVA/Al_2O_3 mixture solution was prepared by using a suitable amount of as-prepared QPVA precipitates, 0–10 wt.%Al_2O_3 fillers, and 5 wt.% GA (a cross-linking agent), 1 vol.%HCl at 85 °C for 3 h under a continuous stirring condition. The resulting viscous blend polymer solution was poured out on a glass plate. The thickness of the wet composite polymer membrane was between 0.020 and 0.040 cm. The glass plate with viscous QPVA/Al_2O_3 composite polymer sample was weighed again and then the excess water was allowed to evaporate slowly at 60 °C at a relative humidity of 30%. After evaporation of water solvent, the glass plate with the composite polymer membrane was weighed again. The composition of QPVA/Al_2O_3 polymer membrane was determined from the mass balance. The thickness of the dried composite polymer membrane was controlled in the range of between 0.010 and 0.020 cm.

2.2. Crystal structure, morphology, and thermal analyses

TGA thermal analysis was carried out using a Mettler Toledo TGA/SDT 851 system. Measurements were carried out by heating from 25 to 600 °C, under N_2 atmosphere at a heating rate of 10 °C min^{-1} with about 10 mg samples. The surface morphology and microstructure of the QPVA/Al_2O_3 nanocomposite polymer membrane were investigated by a scanning electron microscope (SEM) (Hitachi S-2600H).

2.3. Ionic conductivity and methanol permeability measurements

Conductivity measurements were carried out on QPVA/Al_2O_3 nanocomposite polymer electrolytes via an AC impedance method. The QPVA/Al_2O_3 nanocomposite samples were immersed in a 4 M KOH solution for 24 h before measurement. Alkaline QPVA/Al_2O_3 nanocomposite polymer membranes were clamped between stainless steel (SS304), ion-blocking electrodes, each of surface area 1.32 cm^2, in a spring-loaded glass holder. A thermocouple was kept in close proximately to the composite polymer membrane for temperature measurement. Each sample was equilibrated at the experimental temperature for at least 30 min before measurement. AC impedance measurements were carried out using an Autolab PGSTAT-30 equipment (Eco Chemie B.V., Netherlands). The AC spectra in the range of 300 kHz to 10 Hz at an excitation signal of 10 mV were recorded. AC impedance spectra of the nanocomposite polymer membrane were recorded at a temperature range between 30 and 70 °C. Experimental temperatures were maintained within ±0.5 °C by a convection oven. All QPVA/Al_2O_3 nanocomposite polymer electrolytes were examined at least three times.

Methanol permeability measurements [21,22] were conducted by using a diffusion cell. The cell was divided into two compartments, in which one compartment was filled with D.I. water (called B compartment) and the other compartment filled with a 20 wt.% methanol aqueous solution (called A compartment). Prior to testing, the QPVA/Al_2O_3 nanocomposite polymer membrane was hydrated in D.I. water for at least 24 h. The composite polymer membrane with a surface area of 0.58 cm^2 was sandwiched by O-ring and clamped tightly between two compartments. A stir bar was kept active in the glass diffusion cell during the experiment. The concentration of methanol diffused from compartment A to B across the QPVA/Al_2O_3 nanocomposite polymer membrane was examined using a density meter (Mettler Toledo, DE45). An aliquot of 0.20 mL was sampled from the B compartments every 30 min. Before the permeation experiment, a calibration curve for the value of density vs. the methanol concentration was prepared. The calibration curve was used to calculate the methanol concentration in the permeation experiment. The methanol permeability was calculated from the slope of the straight-line plot of methanol concentration vs. permeation time. The methanol concentration in the B compartment as a function of time is given in Eq. (1) [21,22]:

$$C_B(t) = \frac{A}{V}\frac{DK}{L}C_A(t - t_o) \quad (1)$$

where C is the methanol concentration, A and L are the composite polymer membrane area and thickness, D and K are the methanol diffusivity and partition coefficient between the membrane and the solution. The product DK is the membrane permeability (P), t_o, a time lag, is related to the diffusivity (D): $t_o = L^2/6D$.

2.4. Micro-Raman spectroscopy analyses

Micro-Raman spectroscopy is a quick tool to characterize pure PVA and the QPVA polymer membranes. The micro-Raman spectroscopy analysis was carried out using a Renishaw confocal microscopy Raman spectroscopy system with a microscope equipped with 10×, 20×, and 50× objectives, and a charge coupled device (CCD) detector. Raman excitation source was provided by a 632.8 nm He–Ne laser beam, which had the beam power of 17 mW and was focused on the sample with a spot size of about 1 μm in a diameter.

2.5. Preparation of the anode and cathode electrodes

The catalyst slurry ink for the anode was prepared by mixing 70 wt.% PtRu black inks (Alfa, HiSPEC 6000, PtRu black with Pt:Ru = 1:1 at. ratio), 30 wt.% PTFE binder solution (Du pont, 60 wt.% base solution), and a suitable amount of distilled water and alcohol. The resulting PtRu black mixtures were first ultrasonicated for 2 h. The PtRu black inks for the anode were loaded onto a Ti-screen [1,10] by an impregnation method, which was loaded at 1 or 4 mg cm^{-2}. The as-prepared PtRu anode was dried in a vacuum oven at 110 °C for 2 h.

The carbon slurry for the gas diffusion layer of the air cathode was prepared with a mixture of 70 wt.% Shawinigan acetylene black (AB50) with specific surface area of 80 $m^2\ g^{-1}$ and 30 wt.% PTFE solution (Teflon-30 suspension) as a wet-proofing agent and binder. The carbon slurry was coated on the Ni-foam used as a current collector and then pressed under 100 $kg_f\ cm^{-2}$. The gas diffusion layer was then sintered at temperature of 360 °C for 30 min. The catalyst layer of the air cathode was then prepared by spraying a mixture of a 15 wt.% of PTFE solution binder and 85 wt.% of mixed powders consisting of MnO_2 catalyst mixed with BP2000 carbon black (MnO_2:BP2000 = 1:1). The MnO_2/C catalyst loading on the cathode was controlled at 4 mg cm^{-2}. The Ni-foam current collector was 1 cm × 1 cm. The detailed preparation method of the air electrodes has been reported in literature [23].

2.6. Electrochemical measurements

The QPVA/Al_2O_3 nanocomposite polymer membrane was sandwiched between the sheets of the anode and the cathode, and then pressed at 25 °C under 100 $kg_f\ cm^{-2}$ for 5 min to obtain a membrane electrode assembly (MEA). The electrode area of the MEA was about 1 cm^2.

The electrochemical measurements of alkaline DMFC were carried out in a two-electrode system. AC spectra of the DMFC with the frequency range from 100 kHz to 0.01 Hz at an excitation signal of 5 mV were obtained at OCP and 0.40 V. The *E*–*t* and *i*–*t* curves of alkaline DMFC using a QPVA/Al_2O_3 nanocomposite polymer membrane were recorded at a current density of 100 mA cm^{-2} and a constant cell potential of 0.40 V in 4 M KOH + 1–4 M CH_3OH solution fuels at 25 °C, respectively. The polarization (*I*–*V*) and the power density curves of alkaline DMFC with 4 M KOH + 1–4 M CH_3OH solution fuels were obtained at a scan rate of 1 mV s^{-1} at 25 °C. All electrochemical measurements were performed on an Autolab PGSTAT-30 electrochemical system with GPES 4.8 package software (Eco Chemie, The Netherlands). The electrochemical performances of alkaline DMFC using a QPVA/Al_2O_3 nanocomposite polymer membrane and the cathode open to atmospheric air were systematically studied at room temperature and in ambient air [1,2].

3. Results and discussion

3.1. Thermal analyses

Fig. 1 shows TGA curves for pure PVA film, QPVA film and the QPVA/Al_2O_3 nanocomposite membrane, respectively. The TGA curve of pure PVA film shows three major weight loss regions. The first region at a temperature of 80–130 °C ($T_{max,1}$ = 89.1 °C) is due to the evaporation of weakly physical and strongly chemical bound H_2O; the weight loss of the membrane is about 5–6 wt.%. The second transition region at around 240–310 °C ($T_{max,2}$ = 264 °C) is due to the degradation of the PVA polymer film; the total weight loss corresponds to this phase, about 60–70 wt.%. The peak of third stage at around 410–460 °C ($T_{max,3}$ = 439 °C) is due to the cleavage backbone of PVA polymer film; the total weight loss is about 94.63 wt.% at 600 °C.

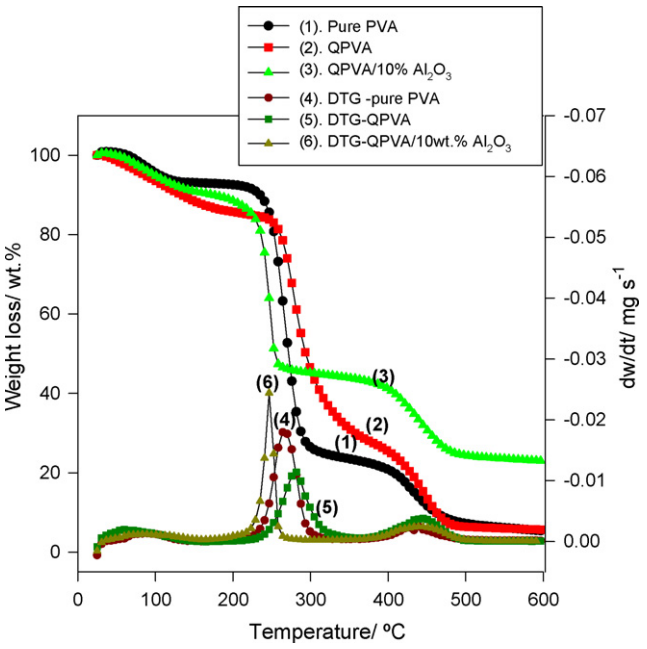

Fig. 1. TGA curves for the pure PVA, QPVA, and QPVA/10%Al_2O_3 polymer membrane.

Fig. 1 also shows TGA curves of the QPVA polymer membrane. The QPVA film also shows three major weight loss regions. The QPVA film, the first region at a temperature of 80–150 °C ($T_{max,1}$ = 89.2 °C) is due to the evaporation of weakly physical and strongly chemical bound water; the weight loss of the membrane is also about 6–7 wt.%. The peak of the second transition at around 250–320 °C ($T_{max,3}$ = 270 °C) is due to the degradation of the PVA polymer membrane. The peak of third stage at 410–470 °C ($T_{max,4}$ = 445 °C) is due to the cleavage of the C–C backbone of QPVA polymer membranes; the total weight loss is about 94.33 wt.% at 600 °C.

Moreover, TGA curve of QPVA/10 wt.%Al_2O_3 nanocomposite polymer membrane also reveals three major weight loss regions, which appear as three peaks in the DTG curves. The first region at a temperature of 80–150 °C ($T_{max,1}$ = 83 °C) is also due to the evaporation of free and bound H_2O; the weight loss of the membrane is ~5 wt.%. The peak of the second transition at around 220–280 °C ($T_{max,3}$ = 246 °C) is also due to the degradation of the QPVA polymer membrane. The peak of the third transition at 420–480 °C ($T_{max,4}$ = 440 °C) is due to the cleavage of the C–C backbone of the QPVA polymer membrane; the total weight loss is only ca. 77 wt.% at 600 °C.

Accordingly, the degradation peaks of cross-linked QPVA/Al_2O_3 nanocomposite polymer membranes are less intense and shift towards higher temperatures. It can be concluded that the thermal stability is improved probably due to the additive effect of Al_2O_3 fillers and the chemical cross-link reaction between QPVA and glutaraldehyde.

3.2. Surface morphology, mechanical properties, and micro-Raman analyses

SEM photographs of the top and cross-section views of the QPVA/10 wt.%Al_2O_3 nanocomposite polymer membranes are shown in Fig. 2(a) and (b), at a magnification of 500×, respectively. It is revealed that the surface morphology of the QPVA/10 wt.%Al_2O_3 nanocomposite polymer sample shows some nt-TiO_2 aggregates or chunks, which are randomly distributed on the top surface. It

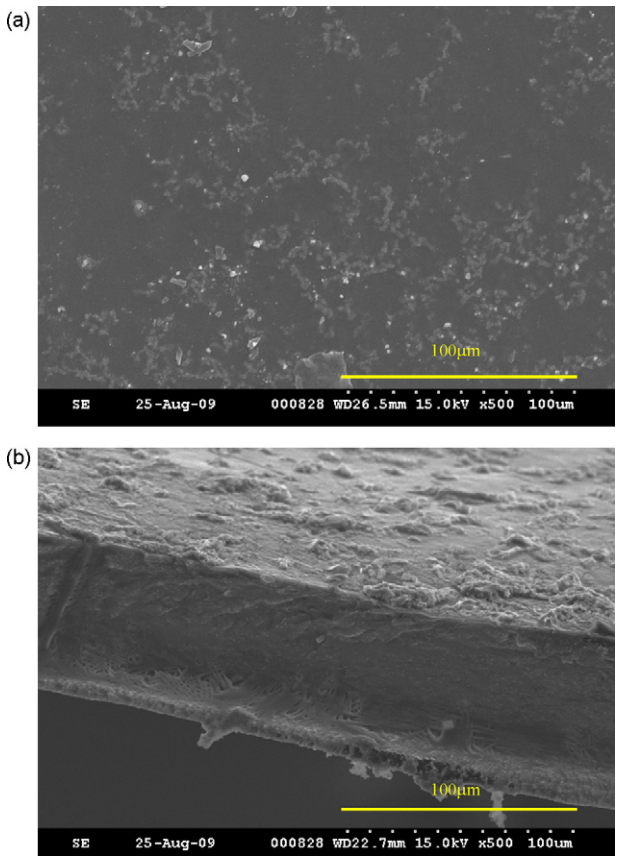

Fig. 2. SEM photographs for QPVA/10 wt.%Al_2O_3 polymer membrane: (a) top-view and (b) cross-view.

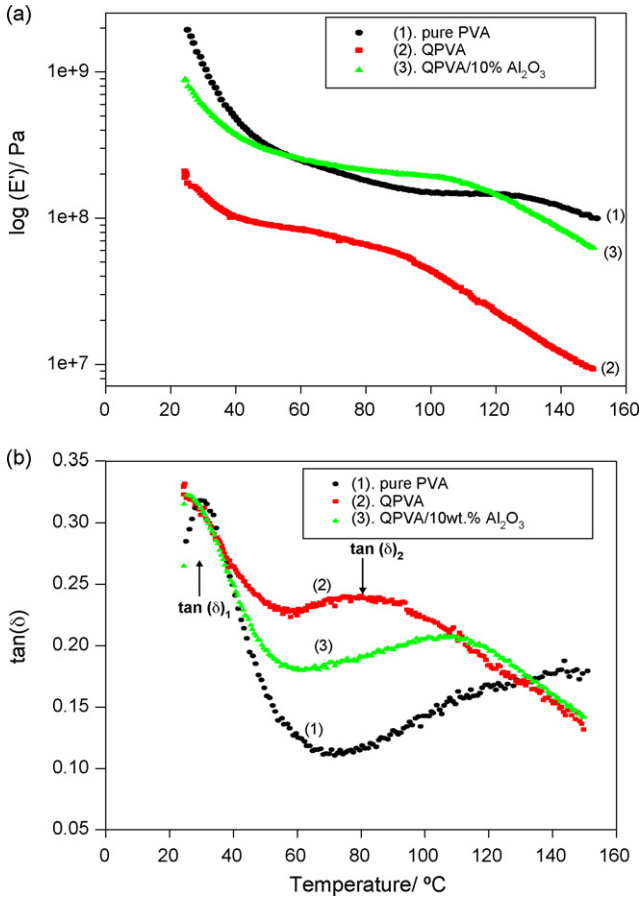

Fig. 3. DMA curves for the pure PVA, QPVA, and QPVA/10%Al_2O_3 nanocomposite polymer membranes: (a) E' vs. T and (b) tan(δ) vs. T.

is found that the dimension of these Al_2O_3 aggregates embedded in PVA matrix is about 1–10 μm. Apparently, as SEM results indicate that these nano-sized Al_2O_3 fillers tend to cause formation of aggregates and thus cause a poor dispersion in the PVA polymer host.

Generally, the hydrophilic PVA polymer and Al_2O_3 fillers are homogeneous and compatible without any phase separation occurred when a suitable amount of Al_2O_3 ceramic fillers are added. As it can be seen, the suitable amount of Al_2O_3 fillers (also used as the methanol permeation barriers) in the polymer network matrix may assist in reducing methanol crossover through the nanocomposite polymer membrane.

Fig. 3(a) shows the storage modulus (E') vs. temperature curves for pure PVA film, QPVA film, and QPVA/10 wt.%Al_2O_3 nanocomposite polymer membrane. The storage modulus of pure PVA film ($E' = 1.13 \times 10^9$ Pa) was higher than those of QPVA film ($E' = 1.44 \times 10^8$ Pa) and QPVA/10 wt.%Al_2O_3 nanocomposite polymer membrane ($E' = 5.99 \times 10^8$ Pa) at 30 °C, as shown in Table 1. It was demonstrated that the storage moduli of QPVA film and the QPVA/Al_2O_3 nanocomposite membranes decrease when the Al_2O_3 fillers are added or the PVA polymer is being quaternized by GTMAC. In fact, the storage modulus of the QPVA/10 wt.%Al_2O_3 polymer membrane at 100 °C ($E' = 1.72 \times 10^8$ Pa) was slightly higher than that of pure PVA film ($E' = 1.51 \times 10^8$ Pa).

Table 1
The results of storage modulus (E') at various temperatures for pure PVA, QPVA, and QPVA/10 wt.%Al_2O_3 nanocomposite polymer membranes at various temperatures.

Types	Pure PVA (Pa)	QPVA (Pa)	QPVA/10 wt.%Al_2O_3 (Pa)
30 °C	1.13×10^9	1.44×10^8	5.99×10^8
60 °C	2.52×10^8	8.45×10^7	2.54×10^8
100 °C	1.51×10^8	4.47×10^7	1.72×10^8
130 °C	1.31×10^8	1.68×10^7	1.12×10^8
140 °C	1.18×10^8	1.19×10^7	8.27×10^7
150 °C	1.07×10^8	9.30×10^6	6.26×10^7
tan(δ)$_1$ peak/°C	30.87	27.27	26.32
tan(δ)$_2$ peak/°C	–	81.18	109.25

Clearly, it was confirmed that these Al_2O_3 fillers markedly enhance the mechanical properties of the QPVA/Al_2O_3 composite polymer membrane. However, when the content of Al_2O_3 fillers was over 10 wt.%, the stiffening effect was progressively decreased due to the serious agglomeration of Al_2O_3 fillers in the PVA polymer matrix.

Fig. 3(b) shows the loss factor or tan(δ) vs. temperature curves for pure PVA film, QPVA film, the QPVA/10 wt.%Al_2O_3 composite film. The glass transition temperatures (T_g) can also be taken at a peak of the tan(δ) curve (denoted as tan(δ)$_1$). The results indicate that the glass transition temperatures of pure PVA film (designated as a $T_{g,PVA}$) and the QPVA/10 wt.%Al_2O_3 SPE are 30.87 and 26.32 °C, respectively. Whereas the glass transition temperatures of the QPVA film and the QPVA/10 wt.%Al_2O_3 SPE (ca. 26–27 °C) are lower than that of pure PVA film (at 30.8 °C). Generally, the sensitivity of the glass transition temperature measurement by DMA is much better than that by DSC. It may be concluded that the actual glass transition temperature of the QPVA/10 wt.% Al_2O_3 composite polymer membrane is around 26–27 °C. Obviously, these quaternized PVA polymer films (i.e., QPVA and QPVA/Al_2O_3) show much lower degree of crystallinity, as compared with pure PVA film.

Furthermore, it was observed that there are two tan(δ) peaks, i.e., tan(δ)$_1$ and tan(δ)$_2$, for QPVA/10 wt.%Al_2O_3 nanocomposite polymer membranes; the variation region of the first tan(δ) peak (i.e., take tan(δ)$_1$ as $T_{g,PVA}$ at 26 °C) is located between 20 and

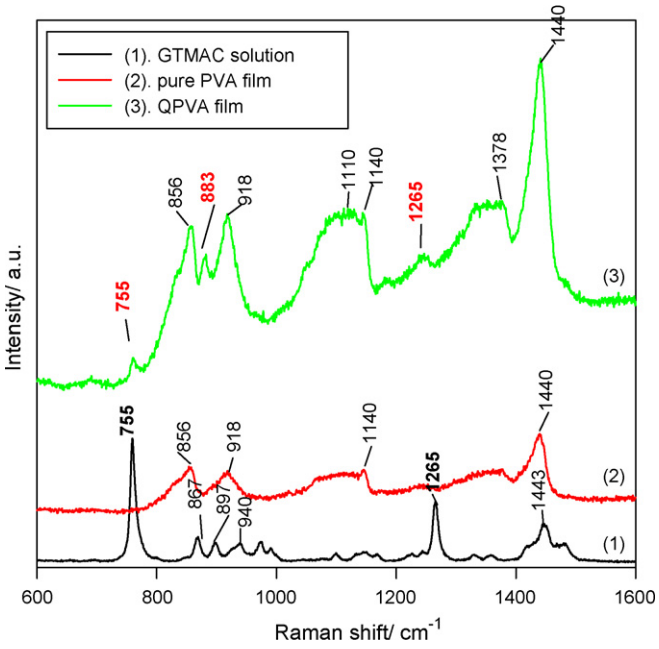

Fig. 4. Micro-Raman spectra for GPTMAC solution, pure PVA, and the QPVA polymer membrane.

60 °C; however, the secondary tan(δ) peak (designated as tan(δ)$_2$) is observed at 109.2 °C, the so-called the β_c relaxation; it is due to the relaxation of the crystalline domain of QPVA/10 wt.%Al_2O_3 nanocomposite polymer membrane. Interestingly, there is no clear tan(δ)$_2$ peak on pure PVA film. Clearly, it was revealed that the degree of crystallinity of QPVA/10 wt.%Al_2O_3 SPE is lower than that of QPVA SPE.

The lower intensity value of the tan(δ)$_2$ peak for the QPVA/10 wt.%Al_2O_3 nanocomposite polymer membrane can be described as the incompatibility within two materials or the decrease in the crystallinity for QPVA/10 wt.%Al_2O_3 SPE. The broader and lowering intensity of tan(δ)$_2$ peaks may be due to the decrease of the crystallinity of the QPVA/10 wt.%Al_2O_3 SPE.

Fig. 4 shows the micro-Raman spectra of GTMAC (used as an animating agent), pure PVA film, and the QPVA film, respectively. There are several strong characteristic scattering peaks for pure PVA film, located at 852, 918, 1140, and 1440 cm^{-1}, respectively. It can be observed from micro-Raman spectra that some characteristic peaks for GTMAC are found at 755, 867, 897, 940, 1265, and 1443 cm^{-1}. In contrast, there are several main peaks for the QPVA film, located at 755, 856, 883, 918, 1110, 1140, 1265, and 1378 cm^{-1}, as seen in Fig. 4. In particular, three Raman characteristic peaks at 755, 883, and 1265 cm^{-1} were appeared on the QPVA film, as compared with the Raman peaks of pure PVA. The peak at 755 cm^{-1} is due to the C–N stretching; the peak at 883 cm^{-1} is identified for C–O–C stretching; the peak of 1265 cm^{-1} could be due to the C–H deformation. It is a proof that PVA polymer has been successfully quaternized by GTMAC via a quaternization process. Table 2 lists several major Raman peak positions for GTMAC, pure PVA film and the QPVA film.

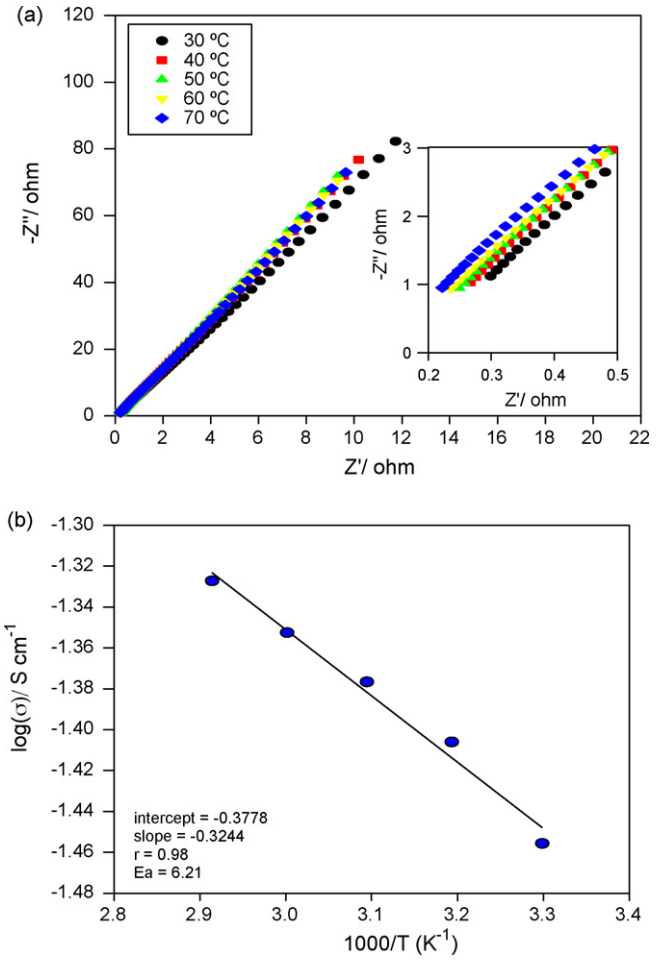

Fig. 5. Nyquist (a) and Arrhenius (b) plots for the QPVA/10 wt.%Al_2O_3 nanocomposite polymer electrolyte in 4 M KOH.

3.3. Ionic conductivity and alcohol permeability measurements

The typical AC impedance spectra of QPVA/10 wt.%Al_2O_3 nanocomposite polymer membrane at different temperatures are shown in Fig. 5(a). The AC spectra were typically non-vertical spikes for stainless steel (SS) blocking electrodes, i.e., the SS|QPVA/Al_2O_3 SPE|SS cell. Analysis of the spectra yielded information about the properties of the QPVA/Al_2O_3 polymer electrolyte, such as bulk resistance, R_b. Taking into account the thickness of the nanocomposite electrolyte films, the R_b value was converted into the ionic conductivity value, σ, according to the equation: $\sigma = L/R_bA$, where L is the thickness (cm) of QPVA/Al_2O_3 polymer membrane, A is the area (cm^2) of the blocking electrode, and R_b is the bulk resistance (ohm) of the alkaline nanocomposite polymer membrane.

Typically, the R_b values of QPVA/10 wt.%Al_2O_3 nanocomposite polymer membranes are on the order of 0.2–0.3 ohm (as seen in the inset of Fig. 5(a)) and are highly dependent on the contents of Al_2O_3 fillers and the concentration of KOH. Note that the nanocomposite

Table 2
Raman peak positions for GTMAC, pure PVA, QPVA polymer membranes.

Types	Peaks								
	Raman major peak positions/cm^{-1}								
GTMAC	755	867	897	940	1265	1443			
Pure PVA	852	918	1140	1440					
QPVA	755	856	883	918	1110	1140	1265	1378	1440

Table 3
Ionic conductivities (S cm^{-1}) of QPVA/Al_2O_3 nanocomposite polymer membranes containing 4 M KOH electrolytes at various temperatures.

Temp.	σ/S cm^{-1}			
	Pure PVA	QPVA/0 wt.%Al_2O_3	QPVA/5 wt.%Al_2O_3	QPVA/10 wt.%Al_2O_3
30 °C	0.0106	0.0137	0.0165	0.0350
40 °C	0.0112	0.0147	0.0183	0.0392
50 °C	0.0131	0.0170	0.0203	0.0420
60 °C	0.0152	0.0195	0.0228	0.0444
70 °C	0.0182	0.0210	0.0247	0.0479

polymer membrane was immersed in a 4 M KOH solution for 24 h before measurement.

Table 3 lists the ionic conductivity values of pure PVA film, QPVA film, and QPVA/10 wt.%Al_2O_3 nanocomposite polymer membrane with a 4 M KOH electrolyte solution at different temperatures. As a result, the ionic conductivity of alkaline pure PVA film is 0.0106 S cm^{-1} at 30 °C. Comparatively, the ionic conductivities of alkaline QPVA/5 wt.%Al_2O_3 and QPVA/10 wt.%Al_2O_3 nanocomposite polymer electrolytes (being soaking in 4 M KOH electrolyte) are 0.0137, 0.0165, and 0.035 S cm^{-1} at 30 °C, respectively. It showed that the highest ionic conductivity of the QPVA/10 wt.%Al_2O_3 nanocomposite polymer electrolyte is σ = 0.0350 S cm^{-1} at ambient temperature. It was also found that the ionic conductivity of the QPVA film ($\sigma_{30\,^\circ C}$ = 0.0137 S cm^{-1}) is higher than that of pure PVA film ($\sigma_{30\,^\circ C}$ = 0.0106 S cm^{-1}) [1,2]. By comparison, the ionic conductivity of QPVA/10 wt.%Al_2O_3 nanocomposite polymer electrolyte ($\sigma_{30\,^\circ C}$ = 0.0350 S cm^{-1}) is higher than that of PVA/10 wt.%TiO_2 composite polymer electrolyte ($\sigma_{30\,^\circ C}$ = 0.0012 S cm^{-1}) [24].

According to the ionic conductivity result, it is seen clearly that the ionic conductivity of QPVA/Al_2O_3 nanocomposite polymer electrolytes increases when the content of Al_2O_3 fillers was increased. As we know, when the Al_2O_3 fillers used as stiffener materials were added to the QPVA matrix, the swelling ratio of QPVA membranes can be effectively reduced (data not shown here). As expected, the thermal and mechanical properties, and dimensional stability are also improved.

However, the ionic conductivity of QPVA/Al_2O_3 nanocomposite polymer electrolytes starts to decrease when the content of Al_2O_3 fillers is over 10 wt.%. From the $\log_{10}(\sigma)$ vs. $1/T$ plots, as shown in Fig. 5(b), the activation energy (E_a) of the QPVA/10 wt.%Al_2O_3 polymer electrolyte can be obtained, which is highly dependent on the contents of Al_2O_3 fillers and KOH concentrations. In addition, the E_a value of the QPVA/10 wt.%Al_2O_3 nanocomposite polymer membranes is on the order of 5~6 kJ mol^{-1}.

Furthermore, the permeability measurements for methanol were carried out on the QPVA/Al_2O_3 nanocomposite polymer membrane. All values of methanol permeability for QPVA/Al_2O_3 nanocomposite polymer membranes were obtained from the slope of the straight line (also see references of [1,2]). It is shown that the methanol permeability values of the QPVA/Al_2O_3 nanocomposite polymer membrane are (6.66–2.81) × 10^{-7} cm^2/s, at 25 °C. However, the permeabilities of the QPVA/Al_2O_3 nanocomposite polymer membranes (on the order of 10^{-7} cm^2 s^{-1}) are lower than that of Nafion membrane (on the order of 10^{-6} cm^2 s^{-1}).

3.4. Electrochemical measurements

The AC impedance spectra of the DMFC using a QPVA/10 wt.%Al_2O_3 nanocomposite polymer membrane with 4 M KOH + *x* M CH_3OH solution fuels at open circuit potential are shown in Fig. 6(a). The area bulk resistance (A_R) is around 0.2–0.40 ohm cm^2, as seen more clearly in the inset of Fig. 6(a) at high frequency region. In addition, AC impedance spectra of the DMFC with 4 M KOH + *x* M CH_3OH solution fuels at 0.40 V are shown in Fig. 6(b). The area bulk resistance is around 0.3–0.40 ohm cm^2, as seen clearly in the inset of Fig. 6(b). The value of the area bulk resistance of the QPVA/10 wt.%Al_2O_3 nanocomposite polymer membrane is comparable to that of Nafion 117 (A_R = 0.35 ohm cm^2) [1].

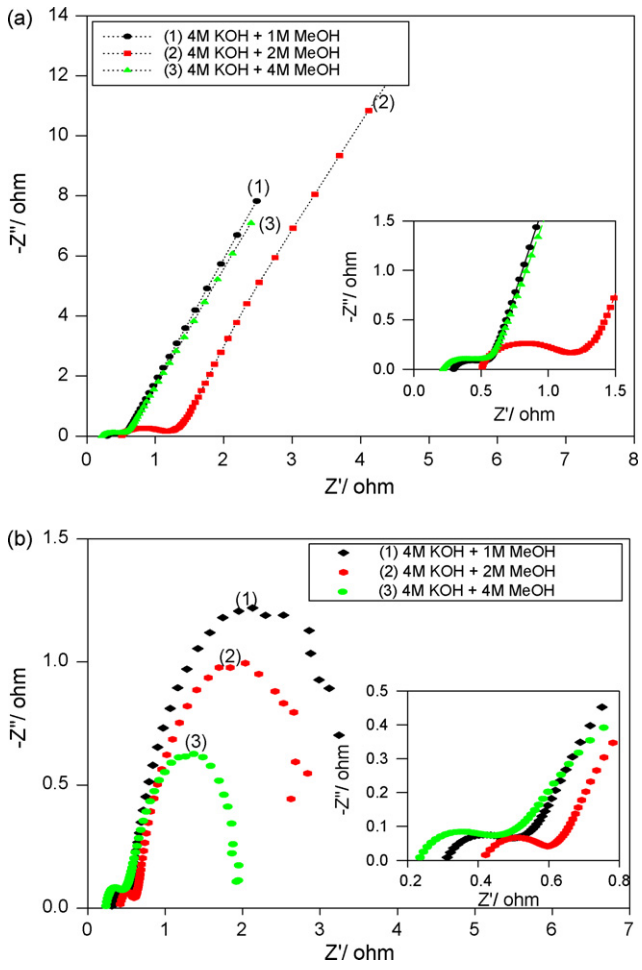

Fig. 6. AC impedance spectra for the DMFC comprised of the QPVA/10%Al_2O_3 polymer membrane with 4 M KOH + *x* M CH_3OH fuels at 25 °C and in ambient air: (a) OCP and (b) 0.40 V.

The *E*–*t* curves of the DMFC with various 4 M KOH + *x* M CH_3OH solution fuels at 25 °C at a constant current density of 100 mA cm^{-2} are shown in Fig. 7. It is observed that the best electrochemical performance of the DMFC is for 4 M KOH + 4 M methanol fuel (E_{avg} = 0.353 V, P.D. = 35.3 mW cm^{-2}); in contrast, the poorest one (E_{avg} = 0.191 V, P.D. = 19.1 mW cm^{-2}) is for 4 M KOH + 1 M methanol fuel. Obviously, the electrochemical performance of the DMFC with fuels in sequence is as follows: 4 M methanol > 2 M methanol > 1 M methanol.

Fig. 8 shows the *i*–*t* curves of the DMFCs consisting of the PtRu anode, the MnO_2 cathode and a QPVA/10 wt.%Al_2O_3 nanocomposite polymer membrane with 4 M KOH + 1–4 M methanol fuels at 0.40 V at 25 °C and in ambient air. The average current densities of the DMFCs with 4 M KOH + 1, 2, and 4 M methanol fuels are 57.14, 75.01, and 98.24 mA cm^{-2}, respectively. In spite of a tendency of the cell potential to drop at the beginning of the test, the current densities remained constant during the test period.

Fig. 9 shows the potential–current density and the power density–current density curves of the DMFCs with 4 M KOH + 1–4 M methanol fuels, respectively. As a result, the highest peak power density of 36.15 mW cm^{-2} for the DMFC with a 4 M KOH + 4 M methanol fuel is achieved at $E_{p,max}$ = 0.235 V with a peak current

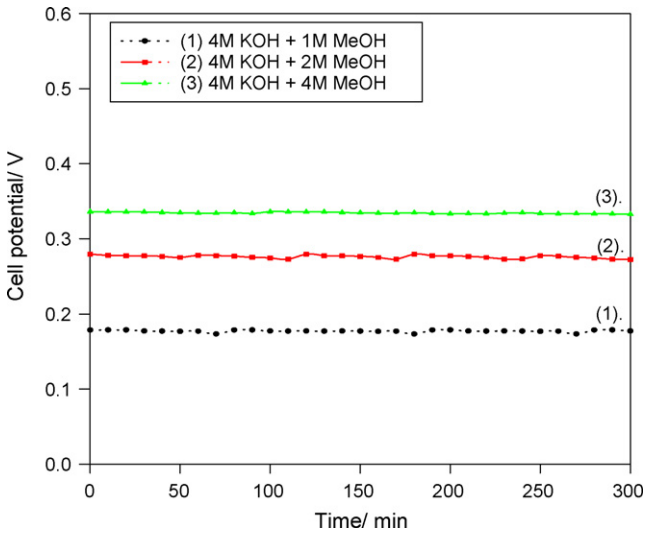

Fig. 7. The *E*–*t* curves for DMFC comprised of QPVA/10 wt.%Al_2O_3 polymer membrane with 4 M KOH + *x* M CH_3OH fuels at 25 °C and in ambient air.

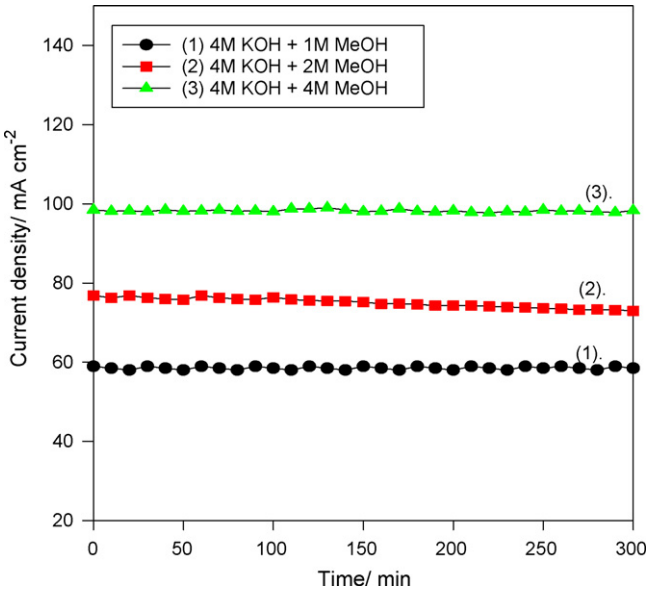

Fig. 8. The *i*–*t* curves for the DMFC comprised of QPVA/10 wt.%Al_2O_3 polymer membrane with 4 M KOH + *x* M CH_3OH fuels at 25 °C and in ambient air.

density ($i_{p,max}$) of 153.53 mA cm^{-2}, as listed in Table 4. On the other hand, the peak power density of alkaline DMFC with a 4 M KOH + 2 M CH_3OH fuel is 32.40 mW cm^{-2} at $E_{p,max}$ = 0.239 V with a peak current density of 135.52 mA cm^{-2} at 25 °C. In comparison, the peak power density of the DMFC using a QPVA/10 wt.%Al_2O_3 membrane with a 4 M KOH + 2 M CH_3OH fuel (P.D.$_{max}$ = 32.40 mW cm^{-2}) is much higher than that of the DMFC using a PVA/10 wt.%TiO_2 membrane (P.D.$_{max}$ = 9.25 mW cm^{-2}) [24] at the same amount cat-

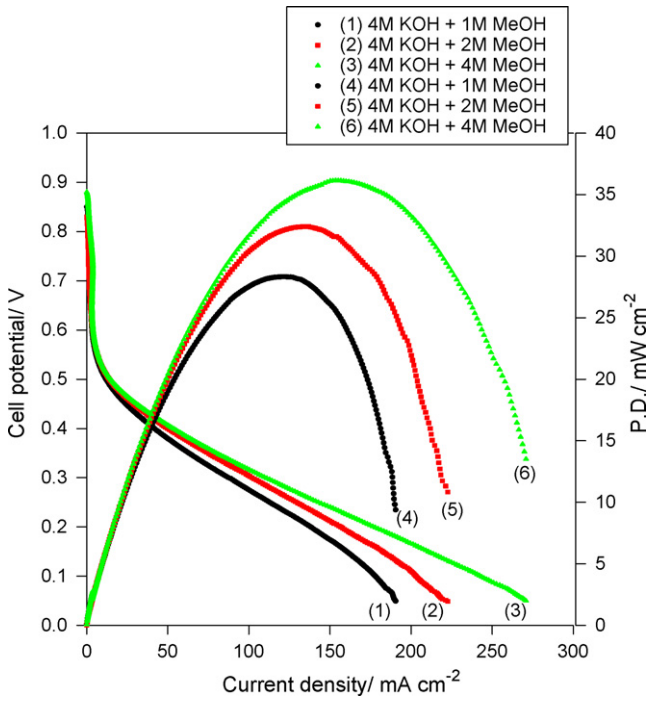

Fig. 9. The *I*–*V* and PD curves the DMFC comprised of QPVA/10 wt.%Al_2O_3 polymer membrane with various 4 M KOH + *x* M CH_3OH fuels at 25 °C and in ambient air.

alyst loadings on the electrodes, i.e., the anode with 4 mg cm^{-2} PtRu black ink and the cathode with 4 mg cm^{-2} MnO_2/C ink. This indicates that the electrochemical performance could be greatly improved (about 3.5 times) via a quaternization process [8–10] on the PVA polymer.

Furthermore, the lowest power density of the DMFC with a 4 M KOH + 1 M CH_3OH fuel is about 28.33 mW cm^{-2} at $E_{p,max}$ = 0.232 V with a peak current density of 121.91 mA cm^{-2} at 25 °C. As a matter of fact, the values of peak power densities are also on the order of 4 M CH_3OH > 2 M CH_3OH > 1 M CH_3OH. Especially, 4 M CH_3OH fuel shows the highest power density (36.15 mW cm^{-2}) among three methanol concentrations.

In addition, the different amounts of PtRu black inks on the anode for the DMFC may significantly affect its electrochemical performance. The DMFC comprised of the anode with a PtRu black loading of 1.1 mg cm^{-2} and with same air cathode and the QPVA/10 wt.%Al_2O_3 composite polymer membrane was assembled and examined for comparison. Table 5 displayed the peak powder density results for the DMFC using the anode with a PtRu black loading of 1.1 mg cm^{-2} with 4 M KOH + 1–4 M methanol fuels at ambient conditions. The peak power density of the DMFC (the anode with a 1.1 mg cm^{-2} PtRu black loading) is only 12.36 mW cm^{-2}, which is much less than that of the DMFC (the anode with a 4 mg cm^{-2} PtRu black loading) when the test was carried out at the same 4 M KOH + 4 M methanol concentration. Table 6 lists some electrochemical test results for the DMFC comprising of the anode

Table 4
The *I*–*V* and power density results for the DMFC (the anode: 4 mg cm^{-2} of PtRu black on Ti-screen) using a QPVA/10 wt.%Al_2O_3 polymer membrane with 4 M KOH + *x* M methanol fuels at 25 °C and in ambient air.

Parameters	*x*		
	1 M CH_3OH	2 M CH_3OH	4 M CH_3OH
P.D.$_{max}$/mW cm^{-2}	28.33	32.40	36.15
$i_{p,max}$/mA cm^{-2}	121.91	135.52	153.53
$E_{p,max}$/V	0.232	0.239	0.235

Table 5
The *I*–*V* and power density results for the DMFC (the anode: 1.1 mg cm^{-2} of PtRu black on Ti-screen) using the QPVA/10 wt.%Al_2O_3 polymer membrane with 4 M KOH + *x* M methanol fuels at 25 °C and in ambient air.

Parameters	*x*		
	1 M CH_3OH	2 M CH_3OH	4 M CH_3OH
P.D.$_{max}$/mW cm^{-2}	9.06	12.53	12.36
$i_{p,max}$/mA cm^{-2}	42.55	60.82	62.44
$E_{p,max}$/V	0.210	0.210	0.200

Table 6
Some electrochemical parameters of the DMFC (the anode: 1.1 mg cm^{-2} of PtRu black on Ti-screen) comprising of a QPVA/10 wt.%Al_2O_3 polymer membrane with *x* M KOH + 4 M methanol fuels at 25 °C and in ambient air.

Fuels	Item			
	OCP/V	$i_{p,max}$/mA cm^{-2}	$E_{p,max}$/V	P.D.$_{max}$/mW cm^{-2}
1 M KOH + 4 M CH_3OH	0.82	42.16	0.20	8.53
2 M KOH + 4 M CH_3OH	0.83	56.76	0.18	10.39
4 M KOH + 4 M CH_3OH	0.84	62.44	0.20	12.36
6 M KOH + 4 M CH_3OH	0.88	88.01	0.20	17.72

at 1.1 mg cm^{-2} PtRu black loading with *x* M KOH (*x*: 1–6 M) + 4 M methanol fuels. It was found that the OCP value of the DMFC increases when the concentrations of KOH electrolyte increase. The peak powder density of the DMFC is also increased from 8.53 to 17.72 mW cm^{-2} when the KOH concentration is increased from 1 to 6 M. In summary, these results indicated that the electrochemical performance of the DMFC was markedly affected by the KOH concentrations and the contents of the PtRu black on the anode.

Accordingly, it demonstrates here that alkaline DMFC consists of the air electrode using non-precious metal catalyst, i.e., cheap MnO_2 catalyst instead of expensive Pt. The metal oxide catalyst of MnO_2 is not only inexpensive but also more tolerant towards crossover, and is active for the reduction of O_2 to OH^- in an alkaline media. Another advantage is that the QPVA/Al_2O_3 nanocomposite polymer membrane is a cheap non-perfluorosulfonated polymer membrane, as compared with an expensive Nafion membrane.

4. Conclusions

The nanocomposite polymer membrane based on the QPVA and Al_2O_3 blends was prepared by a solution casting method. It demonstrates that the ionic conductivity of the PVA polymer membrane greatly increases via an amination process employing GTMAC. Alkaline direct methanol fuel cell comprising of the QPVA/Al_2O_3 nanocomposite polymer membrane was assembled and systematically examined. Among three concentrations methanol fuels, the highest peak power density of the DMFC comprising of the anode with 4 mg cm^{-2} PtRu black with a 4 M KOH + 4 M CH_3OH fuel is about 36.25 mW cm^{-2}. However, the peak power densities of the DMFC were on the order of 4 M CH_3OH > 2 M CH_3OH > 1 M CH_3OH.

From the practical point of view, the QPVA/Al_2O_3 nanocomposite polymer membrane can be prepared by a simple process. The QPVA/Al_2O_3 nanocomposite polymer membrane appears a viable candidate for applications in alkaline DMFCs.

Acknowledgements

Financial support from the National Science Council, Taiwan (Project No: NSC-96-2221-E131-009-MY2) is gratefully acknowledged.

References

[1] C.C. Yang, J. Membr. Sci. 288 (2007) 51–60.
[2] C.C. Yang, S.J. Chiu, W.C. Chien, J. Power Sources 162 (2006) 21–29.
[3] Y. Wang, L. Li, L. Hu, L. Zhuang, J. Lu, B. Xu, Electrochem. Commun. 5 (2003) 662–666.
[4] V. Baglio, A.S. Arico, A.D. Blasi, V. Antonucci, P.L. Antonucci, S. Licoccia, E. Traversa, F.S. Fiory, Electrochim. Acta 50 (2005) 1241–1246.
[5] S. Panero, P. Fiorenza, M.A. Navarra, J. Romanowska, B. Scrosati, J. Electrochem. Soc. 152 (12) (2005) A2400–A2405.
[6] H.Y. Chang, C.W. Lin, J. Membr. Sci. 218 (2003) 295–306.
[7] C. Xu, P.K. Shen, X. Ji, R. Zeng, Y. Liu, Electrochem. Commun. 7 (2005) 1305–1308.
[8] K. Matsuoka, Y. Iriyama, T. Abea, M. Matsuoka, Z. Ogumia, J. Power Sources 150 (2005) 27–31.
[9] J.J. Kang, W.Y. Li, Y. Lin, X.P. Li, X.R. Xiao, S.B. Fang, Polym. Adv. Technol. 15 (2004) 61–64.
[10] E.H. Yu, K. Scott, J. Appl. Electrochem. 35 (2005) 91–96.
[11] L. Li, Y.X. Wang, J. Membr. Sci. 262 (2005) 1–4.
[12] J.R. Varcoe, R.C.T. Slade, Fuel Cell 5 (2005) 187–200.
[13] T.N. Danks, R.C.T. Slade, J.R. Varcoe, J. Mater. Chem. 13 (2003) 712–721.
[14] R.C.T. Slade, J.R. Varcoe, Solid State Ionics 176 (2005) 585–597.
[15] J. Fang, P.K. Shen, J. Membr. Sci. 285 (2006) 317–322.
[16] Y. Xiong, J. Fang, Q.H. Zeng, Q.L. Liu, J. Membr. Sci. 311 (2008) 319–325.
[17] Y. Xiong, Q.L. Liu, A.M. Zhu, S.M. Huang, Q.H. Zeng, J. Power Sources 186 (2009) 328–333.
[18] Y. Xiong, Q.L. Liu, Q.G. Zheng, A.M. Zhu, J. Power Sources 183 (2008) 447–453.
[19] A.A. Mohamad, A.K. Arof, Mater. Lett. 61 (2007) 3096–3099.
[20] S. Sang, J. Zhang, Q. Wu, Y. Liao, Electrochim. Acta 52 (2007) 7315–7321.
[21] B. Bae, D. Kim, J. Membr. Sci. 220 (2003) 75–87.
[22] J. Kim, B. Kim, B. Jung, J. Membr. Sci. 207 (2002) 129–137.
[23] C.C. Yang, S.T. Hsu, W.C. Chien, M.C. Shih, S.J. Chiu, K.T. Lee, C.L. Wang, Int. J. Hydrogen Energy 31 (2006) 2076–2087.
[24] C.C. Yang, S.J. Chiu, K.T. Lee, W.C. Chien, C.T. Lin, C.A. Huang, J. Power Sources 184 (2008) 44–51.